



Power Electronic Systems
Laboratory

© 2022 IEEE

IEEE Transactions on Ultrasonics, Ferroelectrics, and Frequency Control, Vol. 69, No. 4, pp. 1572-1575, April 2022

Multi-Frequency Acoustic Levitation and Trapping of Particles in all Degrees of Freedom

M. Röthlisberger,
G. Schmidli,
M. Schuck,
J. W. Kolar

Personal use of this material is permitted. Permission from IEEE must be obtained for all other uses, in any current or future media, including reprinting/republishing this material for advertising or promotional purposes, creating new collective works, for resale or redistribution to servers or lists, or reuse of any copyrighted component of this work in other works.



Eidgenössische Technische Hochschule Zürich
Swiss Federal Institute of Technology Zurich

Multi-Frequency Acoustic Levitation and Trapping of Particles in all Degrees of Freedom

Marc Röthlisberger, Gabriel Schmidli, Marcel Schuck and Johann W. Kolar

Abstract—Stabilization of the position and orientation of non-spherical, sub-wavelength particles in mid air is required for using acoustic levitation forces in applications such as the automation of micro manufacturing processes, 3D-scanning, and inspection. Acoustic locking has previously been demonstrated by time-multiplexing of different acoustic traps at the same frequency. In this case, the magnitude of the acoustic levitation forces and the stabilizing torque are coupled by the ratio of the durations during which the different traps are applied and cannot be adjusted independently assuming operation at maximum power. This work presents a compact device that uses a method for independently adjusting the vertical trapping forces and the stabilizing torque by using two different ultrasonic frequencies. A 40 kHz vertical standing wave is used to generate levitation forces that counteract the gravitational force. Additionally, a 25 kHz horizontal standing wave is used to generate a tunable stabilizing torque. With this method, objects made from high density materials across a wide range of geometries can be locked acoustically with increased stability compared to state-of-the-art methods. This is demonstrated by locking tin cuboids with a density of 7.3 g/cm^3 and plastic cuboids with average side lengths between 0.9 and 3.5 mm. Experimental results demonstrate torsional spring constants of up to 50 nNm/rad and an orientation stability of $<7.5^\circ$.

Index Terms—Acoustic levitation, ultrasonics, robotics

I. INTRODUCTION

Standing acoustic waves have been used for a long time to suspend objects [1], [2], [3]. Despite a variety of potential applications requiring levitation of asymmetric objects [4], [5], [6], most research focuses on the levitation of spherical objects [7], [8]. Standing acoustic waves exert large forces on objects levitating at its nodes, providing the capability of levitating high density objects [9], [10], [11], [12] and manipulating the levitation position of suspended particles by adjusting the positions of these nodes [7], [13]. However, the generated pressure field is rotationally symmetric around the symmetry axis of the setup, resulting in the tendency of levitated particles to spin around this axis [14], [15], [16].

A. Related Work

The trapping of non-spherical particles in position and orientation has been shown in 2D [17] and recently, a method for generating a torque that acoustically locks the orientation of non-spherical, sub-wavelength particles in mid-air (3D) was demonstrated [5]. The latter uses a single-axis acoustic levitator, that time-multiplexes a standing wave and a twin

trap, for generating high vertical forces and a converging torque that locks the rotation, respectively. Subsequently, this method will be referred to as the switching-in-time (SIT) method. The ratio of the times during which the standing wave and the twin trap are applied can be used to tune the converging torque. However, an increase in torque results in a reduced vertical force for operation at maximum power, which limits the maximum density of the suspended object. Switching between different pressure fields requires two phase shifts of 180° per period for each transducer, resulting in a reduced acoustic power output and a further decreased vertical force during the transition process. With this method, an orientation accuracy of $<10^\circ$ and a torsional spring stiffness of up to 40 nNm/rad can be achieved [5]. Another method for controlling the position and orientation of a levitating sample in 3D has been demonstrated in [18]. This approach uses a large number of transducers and 24 individually controlled channels, resulting in a large and complex device. For many applications, it is sufficient to lock the orientation of the levitated object rather than providing full orientational control, which is demonstrated in this work and requires only two individually controlled channels. It has been shown that ultrasonic waves of different frequencies can be used to superimpose different pressure fields and that their interference is canceled out by time averaging [19]. Consequently, pressure fields of different frequencies can be considered separately.

B. Multi-Frequency Method

This work demonstrates the acoustic trapping of asymmetrical objects in all degrees of freedom by using piezoelectric transducers operating at two distinct frequencies. Subsequently, this is referred to as the multi-frequency (MF) method. A vertical standing wave and a horizontal standing wave are generated simultaneously at $f_1 = 40 \text{ kHz}$ and $f_2 = 25 \text{ kHz}$, respectively. The horizontal standing wave results in a pressure field similar in shape to that of a twin trap [5] and results in high forces. Therefore, it is possible to tune the converging torque by adjusting the acoustic power generated at f_2 , without reducing the vertical force generated by the standing wave at the frequency f_1 . The phase inversion is no longer required, making it possible to acoustically lock objects with densities of up to 7.3 g/cm^3 .

II. METHODS

A vertical standing wave is generated by applying a phase shift of 180° between the transducers arranged in the upper

M. Röthlisberger, G. Schmidli, M. Schuck and J. W. Kolar are with the Power Electronic Systems Laboratory, ETH Zürich, Switzerland (e-mail: roethlisberger@lem.ee.ethz.ch).

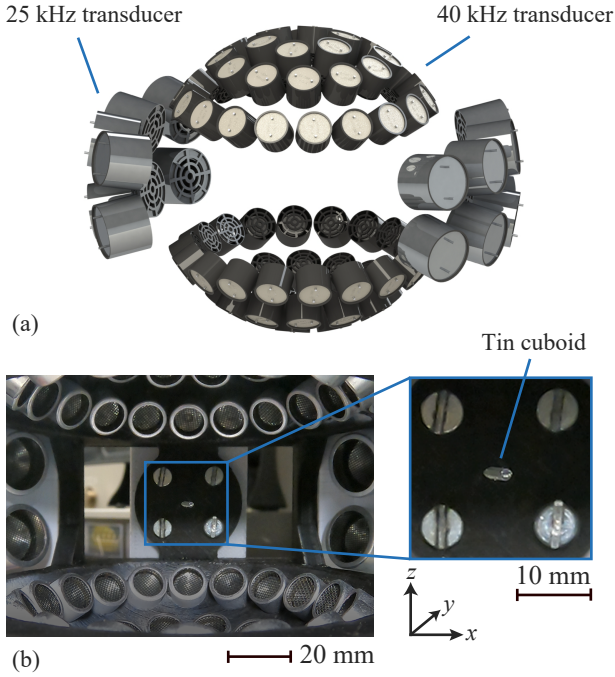


Fig. 1. (a) Rendering of the arrangement with ultrasound transducers with different resonance frequencies and (b) annotated photograph with a levitating tin cuboid. The setup was optimized for providing a maximum converging torque to lock the orientation of the levitated object. The shown acoustically locked object is a tin cuboid with side lengths of 0.8 mm x 0.8 mm x 5 mm.

and lower arrays (cf. Fig. 1) of a single-axis levitator. The resulting pressure field can be calculated as

$$p(x, y, z) = P_0 \sum_i J_0(kr_i \sin \theta_i) \frac{1}{d_i} e^{j\phi_i}, \quad (1)$$

where d_i , ϕ_i , P_0 , J_0 , k , r_i , and θ_i denote the distance of the i^{th} transducer to the considered point (x, y, z) , the phase shift applied to that transducer, a factor depending on the applied voltage, the zeroth-order Bessel function of the first kind, the wave number, the transducer radius, and the angle between the normal of transducer i and the point (x, y, z) , respectively.

A horizontal standing wave is generated at a frequency f_2 without affecting the vertical standing wave if $f_2 \neq f_1$ holds. The resulting acoustic forces acting on a levitated object are obtained from calculating the gradient of the Gor'kov potential U as

$$F = -\nabla U, \quad (2)$$

where

$$U = V_p (K_1 \langle P^2 \rangle - K_2 \langle V^2 \rangle), \quad (3)$$

with $\langle \rangle$, V_p , P , and V denoting time-averaged terms, the particle volume, the pressure, and the particle velocity, respectively. K_1 and K_2 denote factors that depend on the density of the levitating object and the medium as well as the speed of sound in the levitating object and the medium (air). The superposition of Gor'kov potentials of acoustic fields generated using different frequencies is calculated as

$$U_{\text{tot}} = V_p \left(K_1 \langle (P_1 + P_2)^2 \rangle - K_2 \langle (V_1 + V_2)^2 \rangle \right). \quad (4)$$

Due to the orthogonality of sine waves of distinct frequencies, the time-averaged terms can be simplified as

$$\langle (P_1 + P_2)^2 \rangle = \langle P_1^2 \rangle + \langle P_1 P_2 \rangle + \langle P_2^2 \rangle = \langle P_1^2 \rangle + \langle P_2^2 \rangle \quad (5)$$

and

$$\langle (V_1 + V_2)^2 \rangle = \langle V_1^2 \rangle + \langle V_1 V_2 \rangle + \langle V_2^2 \rangle = \langle V_1^2 \rangle + \langle V_2^2 \rangle. \quad (6)$$

A phase difference between the individual pressure fields does not affect the time-averaged pressure field. Consequently, the Gor'kov potential of two superimposed pressure fields of different frequencies is simply the sum of the individual Gor'kov potentials

$$U_{\text{tot}} = U_1 + U_2. \quad (7)$$

This is illustrated in Fig. 2, where a 40 kHz vertical standing wave a), b) is superimposed with a 25 kHz horizontal standing wave c), d), resulting in a Gor'kov potential that is no longer rotationally symmetrical in the xy plane e), f). The equipotential lines of this Gor'kov potential can be approximated by ellipses. The eccentricity of these ellipses, i.e., the ratio of their semi-major and semi-minor axis lengths a and b , respectively, provides a measure for the converging torque.

A. Experimental Setup

For the conducted experiments, an arrangement as shown in Fig. 1 was used. Electroacoustic transducers with a resonance frequency at 40 kHz and a diameter of 10 mm (Manorshi, MSO-A1040H07T) are arranged on three concentric rings of 6, 12, and 18 transducers, respectively. Two such arrays form the pole caps of a sphere with a diameter of 84 mm, i.e., the distance of an object levitated at the center of the arrangement to every transducer is identical, such that high vertical forces can be achieved. Additionally, 16 transducers with a resonance frequency at 25 kHz and a diameter of 16 mm (Manorshi, MSO-A1625H12T) are placed on two concentric rings with a diameter of 100 mm around the symmetry axis of the setup. These rings are arranged at different vertical positions and the transducers are oriented such that they face the center of the arrangement. The setup was designed to maximize the converging torque, i.e., the asymmetry of the Gor'kov potential in the horizontal plane. The asymmetry of the Gor'kov potential was assessed by numerical calculations for different arrangements and numbers of transducers. For the selected arrangement, the resulting Gor'kov potentials correspond to those shown in Fig. 2.

For each frequency, two inverted signals are required to excite the transducers on opposite sides of the arrangement. These signals were generated using a Cyclone II FPGA board and amplified by an L298N dual H-bridge board. The phase of all transducers remains constant during operation, resulting in considerably higher acoustic power compared to the SIT method. Other methods require a large number of individually controlled channels [18], [20], [21] or careful geometric design [22].

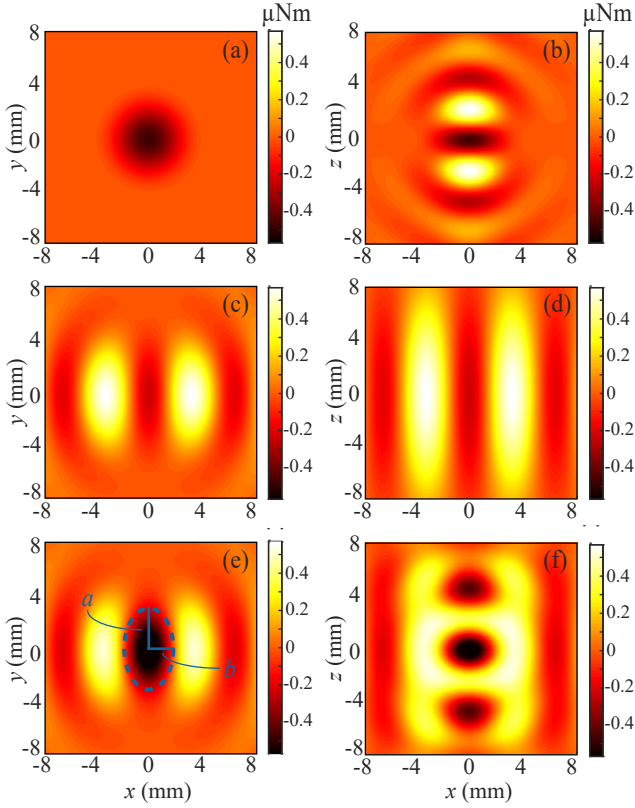


Fig. 2. Top view a) and side view b) of the Gor'kov potential generated by transducers operated at $f_1 = 40$ kHz with a voltage of $V_{1,RMS} = 12$ V. Top view c) and side view d) of the Gor'kov potential generated by transducers operated at $f_2 = 25$ kHz with a voltage of $V_{2,RMS} = 20$ V. Top view e) and side view f) of the superposition of the two Gor'kov potentials with a voltage ratio of $V_2/V_1 = 1.67$, providing high vertical forces and a converging torque. The eccentricity of the equipotential ellipse (dashed line) shown in e) is $a/b = 2.69$.

III. RESULTS

Experiments with 3D-printed cuboids with an aspect ratio of 5:5:3 were conducted to analyze the size range for which stable locking is possible and to measure the orientation stability. Stable locking was defined in accordance with [5] as a maximum oscillation amplitude of 10° and a net zero location and orientation change. The orientation of the levitated cuboids was determined using video footage of the experiments and the Image Processing Toolbox in MATLAB. The obtained orientation stability is shown in Fig. 3a) for plastic cuboids with average side lengths between 0.9 mm and 3.5 mm. Trapping forces of $7.7 \mu\text{N}$, $3.43 \mu\text{N}$, and $9.72 \mu\text{N}$ were achieved for the 0.9 mm object and $453 \mu\text{N}$, $202 \mu\text{N}$, and $572 \mu\text{N}$ for the 3.5 mm object in x , y , and z direction, respectively.

The torsional spring constant K_T was obtained based on the oscillation frequency ω_0 of the locked object, where ω_0 was again determined from video footage. K_T was then calculated as

$$K_T = \omega_0^2 \frac{m}{12} (L_{\text{long}}^2 + L_{\text{short}}^2), \quad (8)$$

where m , L_{long} , and L_{short} denote the mass, the longer side length, and the shorter side length of the cuboid, respectively.

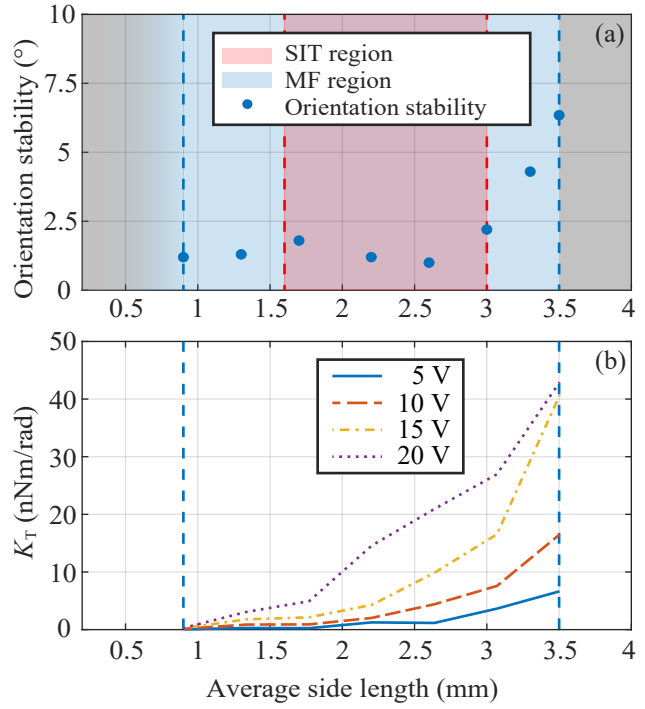


Fig. 3. a) Range of average side lengths of plastic cuboids, that can be locked acoustically using the MF method (blue), compared to the SIT method (red). The measured orientation stability for the MF method is shown by blue dots. b) Measured torsional spring constants for the MF method with voltages from 5 V to 20 V applied to the 25 kHz transducers.

For the cuboids used in the experiments, $L_{\text{long}} = L_{\text{short}}$, thus Eq. 8 can be simplified to

$$K_T = \omega_0^2 \frac{m}{6} L^2. \quad (9)$$

The torsional spring constant depends on the size of the cuboid and the voltage applied to the 25 kHz transducers (acoustic power) as shown in Fig. 3b). If the magnitude of the 25 kHz pressure field approaches the same range as that of the 40 kHz pressure field, the object starts to wobble around the horizontal symmetry axis due to the increased rotational symmetry of the pressure field in Fig. 2f. Therefore, a limit of 20 V was chosen for the voltage applied to the 25 kHz transducers.

The smallest object used for the experiments was a cuboid with an average side length of 0.9 mm. The results show that small objects achieve high orientation stability. Thus, it is expected that the lower limit for the average side length is significantly below 0.9 mm. For cuboids with average side lengths above 3.5 mm, oscillations around horizontal axes cause instabilities or even the ejection of the levitated particle from the acoustic trap. All cuboids between 0.9 mm and 3.5 mm were locked with an orientation stability better than 7.5° . As shown in [5], the approximation of the torque by a torsional spring is valid for oscillation amplitudes α smaller than 15° . The maximum torque for the system demonstrated in this work can therefore be calculated as $T = \alpha K_T$.

The achievable vertical forces were evaluated experimentally using small tin cuboids. Using the MF method, we have

demonstrated acoustic locking of a tin cuboid with side lengths of 0.8 mm x 0.8 mm x 5 mm (average side length of 2.2 mm) and a density of $\rho = 7.3 \text{ g/cm}^3$, as shown in Fig. 1. An oscillation frequency of 5 Hz was measured resulting in a calculated torsional spring constant of 49.3 nNm/rad.

IV. CONCLUSION

The MF and SIT methods can both be used for compact devices with a low complexity compared to methods that control the position and orientation of the levitated sample. The MF method provides a large stability region ranging from average side lengths of 0.9 mm to 3.5 mm, which corresponds to an increase of 86 % compared to the SIT method. Operation of the 40 kHz transducers at full power and no losses due to phase changes during time-multiplexing facilitates the levitation of objects with a density of up to 7.3 g/cm^3 , which is roughly 6 times higher than the maximum density of 1.18 g/cm^3 achieved with the SIT method [5]. However, the MF method device requires laterally placed emitters, which is not the case with the SIT method. The attainable stiffness for both methods is in the range of 40-50 nNm/rad. Control of the system requires two channels of different frequency with constant phase, whereas the SIT method requires four channels of the same frequency with adjustable phase. The efficiency is higher, as the transducers are operated at constant phase. This facilitates the application of the MF method to novel use cases such as the transport of non-spherical objects by contactless robotic grippers or the inspection of acoustically levitated samples.

ACKNOWLEDGMENT

This research was supported by Arbeitsgemeinschaft Prof. Hugel and the ETH Zurich Foundation.

REFERENCES

- [1] A. Kundt, "Über eine neue Art akustischer Staubfiguren und über die Anwendung derselben zur Bestimmung der Schallgeschwindigkeit in festen Körpern und Gasen," *Annalen der Physik*, no. 203.4, p. 497–523, 1866.
- [2] L. V. King, "On the acoustic radiation pressure on spheres," *Proceedings of the Royal Society of London, Mathematical and Physical Sciences*, no. 147.861, pp. 212–240, 1934.
- [3] D. Foresti, M. Nabavi, M. Klingauf, A. Ferrari, and D. Poulikakos, "Acoustophoretic contactless transport and handling of matter in air," *Proceedings of the National Academy of Sciences*, vol. 110, no. 31, pp. 12549–12554, 2013. [Online]. Available: <https://www.pnas.org/content/110/31/12549>
- [4] M. Röthlisberger, M. Schuck, L. Kulmer, and J. W. Kolar, "Contactless picking of objects using an acoustic gripper," *Actuators*, vol. 10, no. 4, 2021. [Online]. Available: <https://www.mdpi.com/2076-0825/10/4/70>
- [5] L. Cox, A. Croxford, B. W. Drinkwater, and A. Marzo, "Acoustic lock: Position and orientation trapping of non-spherical sub-wavelength particles in mid-air using a single-axis acoustic levitator," *Applied Physics Letters*, vol. 113, no. 5, p. 054101, 2018. [Online]. Available: <https://doi.org/10.1063/1.5042518>
- [6] J. Nakahara, B. Yang, and J. R. Smith, "Contact-less manipulation of millimeter-scale objects via ultrasonic levitation," *2020 8th IEEE RAS/EMBS International Conference for Biomedical Robotics and Biomechatronics (BioRob)*, pp. 264–271, 2020. [Online]. Available: <https://doi.org/10.1109/BioRob49111.2020.9224384>
- [7] A. Marzo, T. Corkett, and B. W. Drinkwater, "Ultrasound: An open phased-array system for narrowband airborne ultrasound transmission," *IEEE Transactions on Ultrasonics, Ferroelectrics, and Frequency Control*, vol. 65, no. 1, pp. 102–111, 2018.

- [8] Z. Hong, J. Yin, W. Zhai, N. Yan, W. Wang, J. Zhang, and B. Drinkwater, "Dynamics of levitated objects in acoustic vortex fields," *Scientific Reports*, vol. 7, 12 2017.
- [9] S. Baer, M. A. B. Andrade, C. Esen, J. C. Adamowski, and A. Ostendorf, "Development of a single-axis ultrasonic levitator and the study of the radial particle oscillations," *AIP Conf. Proc.*, vol. 1433, p. 35, 2012.
- [10] R. R. Whymark, "Acoustic field positioning for containerless processing," *Ultrasonics*, vol. 13, p. 251, 1975.
- [11] E. H. Brandt, "Acoustic physics: Suspended by sound," *Nature*, vol. 413, p. 474, 2001.
- [12] M. A. B. Andrade, T. S. Ramos, F. T. A. Okina, and J. C. Adamowski, "Nonlinear characterization of a single-axis acoustic levitator," *Rev. Sci. Instrum.*, vol. 85, p. 045125, 2014.
- [13] A. Marzo, A. Barnes, and B. W. Drinkwater, "Tinylev: A multi-emitter single-axis acoustic levitator," *Review of Scientific Instruments*, vol. 88, no. 8, p. 085105, 2017. [Online]. Available: <https://doi.org/10.1063/1.4989995>
- [14] A. Santillán, K. Volke-Sepulveda, and R. Boullosa, "Acoustically controlled rotations of a disk in free field," *14th International Congress on Sound and Vibration 2007, ICSV 2007*, vol. 5, pp. 4003–4010, 01 2007.
- [15] V. Vandaele, A. Delchambre, and P. Lambert, "Acoustic wave levitation: Handling of components," *J. Appl. Phys.*, vol. 109, p. 124901, 2011.
- [16] Q. Xiu-Pei, G. De-Lu, H. Zhen-Yu, and W. Bing-Bo, "Rotation mechanism of ultrasonically levitated cylinders," *Acta Phys. Sin.*, vol. 66, p. 124301, 2017.
- [17] T. Schwarz, P. Hahn, G. Petit-Pierre, and J. Dual, "Rotation of fibers and other non-spherical particles by the acoustic radiation torque," *Microfluidics and Nanofluidics*, vol. 18, no. 1, pp. 65–79, 2015. [Online]. Available: <https://doi.org/10.1007/s10404-014-1408-9>
- [18] P. Helander, T. Puranen, A. Meriläinen, G. Maconi, A. Penttilä, M. Gritsevich, I. Kassamakov, A. Salmi, K. Muinonen, and E. Hæggeström, "Omnidirectional microscopy by ultrasonic sample control," *Applied Physics Letters*, vol. 116, no. 19, p. 194101, 2020. [Online]. Available: <https://doi.org/10.1063/5.0002602>
- [19] T. Puranen, P. Helander, A. Meriläinen, G. Maconi, A. Penttilä, M. Gritsevich, I. Kassamakov, A. Salmi, K. Muinonen, and E. Hæggeström, "Multifrequency acoustic levitation," in *2019 IEEE International Ultrasonics Symposium (IUS)*, 2019, pp. 916–919.
- [20] A. Marzo, S. A. Seah, B. W. Drinkwater, D. R. Sahoo, B. Long, and S. Subramanian, "Holographic acoustic elements for manipulation of levitated objects," *Nat. Commun.*, vol. 6, p. 8661, 2015.
- [21] A. Marzo, M. Caleap, and B. W. Drinkwater, "Acoustic virtual vortices with tunable orbital angular momentum for trapping of mie particles," *Phys. Rev. Lett.*, vol. 120, p. 044301, 2018.
- [22] A. Marzo, A. Ghobrial, L. Cox, M. Caleap, A. Croxford, and B. W. Drinkwater, "Realization of compact tractor beams using acoustic delay-lines," *Appl. Phys. Lett.*, vol. 110, p. 014102, 2017.